Critically Twisted Kinematic Chains

May 2020

Joint Bachelor Thesis for Degrees in

MATHEMATICS
and
ENGINEERING PHYSICS

Martín Forsberg Conde

Under the kind guidance of

Prof. Eliot Fried
and
Dr. Johannes Schönke
at
Okinawa Institute of Science and Technology

Abstract

Möbius kaleidocycles are a newly discovered family of underconstrained linkages with one degree of freedom. We present many new kinematic chains with similar properties and look for special cases. We give a plausibility argument for the mobility of our chains based on a new theorem on the transposition of adjacent links. Finally, we discuss the relationship between our systems and the emerging field of discrete differential geometry.

Keywords: Mechanisms, Kinematic Chains, Linkages, Kaleidocycles, Discrete Differential Geometry

MSC2020: 53A70, 70B15

Contents

1 Introduction

In this section we present some introductory material on the theory of mechanisms in a broad sense, up to the point where we can give a description of the classical kaleidocycle with 6 links. We do not use the usual mechanical engineering tools for mechanisms in this work, so we will not discuss them in detail. Instead we will quickly describe kaleidocycles and underconstrained chains.

Kinematic chains: A kinematic chain is a collection of rigid bodies (*links*) connected by kinematic pairs (*joints*) so that their motion is restricted. We typically refer to them simply as chains. They are widely used in engineering, and especially in robotics. Typical examples include a robot's arm and the four-bar linkage that allows tractors to lift heavy weights.

Revolute pair: A revolute pair constrains two links to share an axis called a *hinge*. If one of the links is held still, the other one is confined to rigid rotations around the hinge, a one-dimensional motion (compared to the six-dimensional motion for an unconstrained rigid body). For instance, a door is connected to its frame via a revolute pair. While kinematic pairs can be more general, we do not discuss chains featuring other pairs.

Mobility Formula: When computing the degrees of freedom of a chain, we do not count rigid motions that may act on the whole chain. Under this convention, a chain made up of a single rigid body would have no degrees of freedom. The mobility of an N-link chain with R revolute pairs typically follows the formula $f = 6N - 5R - 6$. That is, six degrees of freedom for every rigid body, take five away for every revolute pair, and take six away corresponding to rigid body motions. For instance, the mobility of an N-link open chain is $f = N - 1$, and the mobility of a closed N-link chain (usually called a *linkage*) is usually $f = N - 6$.

The mobility Jacobian: If we want to know how a chain moves, it is natural to do a linear analysis. A chain has a Jacobian, a matrix that describes this linear behavior and can be computed easily as its columns are the Plücker coordinates of the hinges. Its column space corresponds to the tangent space of virtual movements that the last hinge can perform while leaving the first link fixed. An introductory description is given by Angeles [1].

Overconstrained linkages: The most commonly studied exceptions to the previously stated mobility formulas are overconstrained linkages. The mobility of overconstrained linkages with N revolute pairs exceeds the prediction $f = N - 6$. If the first link is fixed, then the last hinge must also be fixed, since it connects to the first link. This means that the possible motions are given by the null space of the Jacobian. The mobility formula for closed linkages can therefore be read as $\dim(N(J)) = N - 6$. This results holds for full rank matrices; however, in overconstrained systems, $\dim(N(J)) > N - 6$. It is not sufficient to satisfy this condition at a point. It should be satisfied throughout the motion of the mechanism in order for it to be overconstrained. This global condition complicates the problem of checking whether a linkage is overconstrained, but it was achieved by Tsai and Morgan [2], leading to the discovery of more examples by Mavroidis and Roth [3].

Underconstrained chains: Less studied exceptions to the mobility formula include underconstrained chains. These mechanisms have less degrees of freedom than predicted. In this case a linear analysis might agree with the mobility formula, or even predict an overconstrained linkage, but a higher order analysis shows that some of the virtual degrees of freedom are inaccessible. The higher-order nature of this relationship means that these chains are usually very sensitive to constraint variations due to construction imprecision, elasticity, thermal expansion, or other factors. Another reason why they have not been studied as much as overconstrained chains is the lack of interesting examples in the literature, within which the only nontrivial mobile example so far are Möbius kaleidocycles, discovered by Schönke and Fried [4]. We hope that the abundance of new mobile examples with novel properties described in this thesis will arouse the interest of the mechanics community.

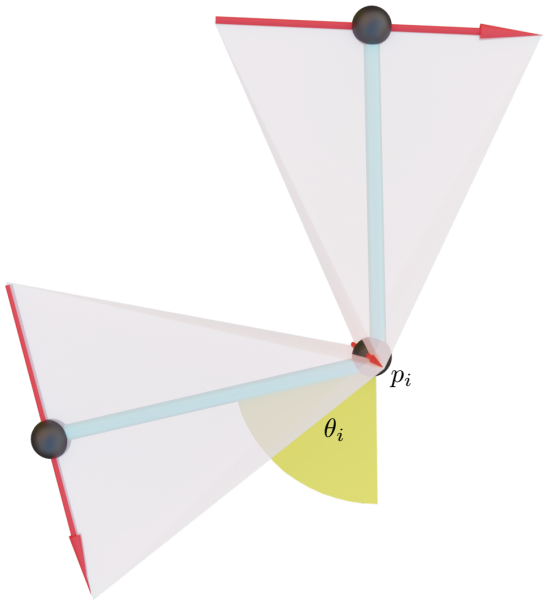

Figure 1: A revolute pair connecting two links. This pair provides a degree of freedom in the form of a rotation around hinge i, the configuration of which is quantified with the angle θ_i. The blue lines are the common perpendiculars to consecutive hinges. In a general rotational pair these lines do not necessarily intersect, but they do meet in the chains we will study. We call the intersection points p_i hinge midpoints, and they form a discrete curve.

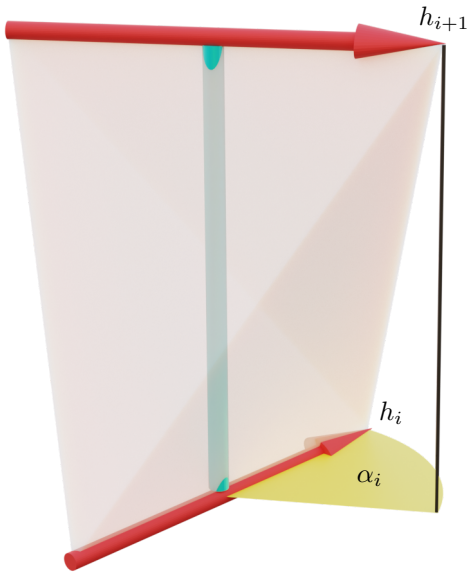

Figure 2: The twist angle α_i of link i betweek hinges i and $i+1$ is angle α_c

Chain parameters: In a chain, the angle and distance between two consecutive hinges is fixed throughout the motion. We write α_i for the angle between hinges i and $i+1$, and l_i for the distance between them. Sometimes it is useful to work with $a_i = \cos\alpha_i$ instead of α_i.

Kaleidocycles: It is possible to close a chain of six links with $\alpha_i = \pi/2$, $i = 1, \cdots, 6$ connected by hinges, thereby creating a linkage with one degree of freedom. This linkage is a classic example of an overconstrained mechanism. It is a special case of a family of mobile 6-link linkages found in 1927 by Bricard [5]. Here are some of its geometrical properties.

1. The linkage exhibits three-fold symmetry with respect to an axis in any configuration.
2. The midpoints of the hinges form an equilateral triangle in one configuration and are part of a cube's vertices in another.
3. The distance between two opposite hinge midpoints is always the same and the hinges always lie in a common plane. The Schatz linkage, which can be used as a mixing machine, is based on this property.
4. The product of the distances from the hinge midpoints to the axis of symmetry is constant.
5. It is possible to move the linkage so that the symmetry axis is left fixed and the hinges are constrained to planes that include this axis.
6. Under this particular motion, the midpoints of the hinges move in their respective planes according to a polyzomal curve of Bernoulli.

Most of these facts were known by Bricard, but points 4 and 6 were established as part of this thesis.

2 Möbius kaleidocycles

This section is a brief description of the most relevant points in [4].

Möbius kaleidocycles are a recently discovered family of underconstrained linkages. They are made up of $N \geq 7$ equal links, so l_i and α_i do not depend on i. We characterize them by their hinge unit vectors h_i, $i = 1, \cdots, N+1$, and we ask that they close non-orientably. Then they must satisfy the following system of $2N + 5$ equations, which we will use extensively from now on:

$$\begin{cases} h_i \cdot h_i & = & 1, & (1.1) \\ h_i \cdot h_{i+1} & = & a, & (1.2) \\ \sum_{i=1}^{N} h_i \times h_{i+1} & = & 0, & (1.3) \\ h_{N+1} & = & -h_1. & (1.4) \end{cases} \tag{1}$$

Here (1.1) holds for $i = 1, \cdots, N+1$ and (1.2) holds for $i = 1, \cdots, N$. (1.1) ensures that h_i are unitary, (1.2) that each link of the chain has twist $\alpha = \arccos a$ and (1.3) and (1.4) ensure that the chain closes non-orientably. When solving this system numerically, we find that for any $N \geq 7$, it has solutions in the real interval $[0, a_c]$, where a_c is the maximum value that a can attain, which also gives α_c, the minimum twist angle. It is a matter of numerical experiment linkages obtained when setting $a = a_c$ have a single degree of freedom. These critically twisted mechanical linkages are called Möbius kaleidocycles.

This result is unexpected. When setting $a = a_c$, we make the linkage underconstrained, and underconstrained linkages are typically immobile. This is actually the first nontrivial example of a mobile underconstrained linkage, conserving this property through its everting motion. It does not fit with the mobility formula $f = N - 6$ either, as the number of degrees of freedom found is 1 regardless of $N \geq 7$.

It is possible look at the midline defined by the vectors $h_i \times h_{i+1} = t_i$ (or by the hinge midpoints p_i) as a discrete framed curve in space, where the hinge vectors h_i are the binormals. It is then possible to compute the self-linking number of this curve, and for all $N \geq 7$ we always find it to be $\mathrm{Lk} = 3$, corresponding to a 3π-twist Möbius band. In the limit $N \to \infty$ we get a continuous curve and the constant twist angle is replaced by a uniform torsion condition.

When $N \geq 7$ is a multiple of 3, the linkages we find are 3-fold symmetric with respect to an axis in every configuration. When $N \geq 7$ is not a multiple of 3, there is not an obvious symmetry axis for any particular configuration. However, because of the symmetry of the linkage, there is a frame of reference where all the hinges follow the same path except for a rotation about an axis and a change of phase. Because of this constant difference in phase between the motion of different hinges, the motion of the kaleidocycle can be thought of as a discrete wave.

Numerics: To find a solution of the system (1) for some particular a one can simply use Newton's method. While the Jacobian is not square, we can use its generalized Penrose inverse in our calculations. This method also shows whether or not there are any solutions for some particular a. We can use this test to perform a binary search on a and find its maximal possible value a_c.

One degree of freedom: Now we give a numerical method to check whether a linkage governed by system (1) locally has one degree of freedom. Configurations are given by the ordered sequence (h_i), $i = 1, \cdots, N+1$ of unit-length hinges. The configuration space is the $(3N + 3)$-dimensional vector space consisting of those points given by the components of (h_i). We supply this vector space

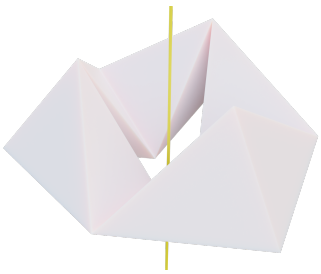

Figure 3: The classical 6-link kaleidocycle in a general configuration. It shows threefold symmetry with respect to the yellow axis.

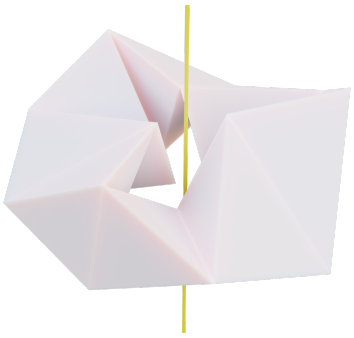

Figure 4: A Möbius kaleidocycle with 9 links. It has a critical twist of $\alpha_c \approx 0.3010\pi$. Whereas the mobility formula would predict three degrees of freedom, this linkage has exactly one degree of freedom.

with the usual Euclidean metric so that distances between configurations are well-defined. Now, after fixing enough components of (h_i) to forbid rigid rotations, we look for solutions at a small distance ϵ from a given starting configuration. If we find none, then the linkage is immobile. If we find only two solutions, then the linkage locally has one degree of freedom. If we find many solutions, the linkage locally has more than one degree of freedom.

3 Irregular kaleidocycles

Now that we know about Möbius kaleidocycles, we begin our research by seeking generalizations of this family of linkages.

3.1 Kaleidocycles with a disparate link

We are interested in finding other underconstrained chains that feature a one-dimensional motion. Let us start by restricting ourselves to linkages and asking that one of the $N \geq 7$ links, say the first, has a different length $l' \neq l$, while still demanding that all twist angles be the same. For any such l' we can still compute the critical twist angle α_c of the links via a binary search. When we do this, we find that our new mechanisms are immobile. A reasonable guess would be that for the linkage to be mobile the disparate link with $l' \neq l$ should have a different twist angle $\alpha'_c \neq \alpha_c$, but it is not clear how to find it.

We now look for an α'_c that gives a linkage with a degree of freedom. We seek a continuous function $s(\alpha')$ such that $s(\alpha'_c) = 0$ when the linkage with α'_c is mobile. Once we have the function s, we can perform a Newton's method or a ternary search in order to find its zeros. To find one such s, let us add some constraints in our Newton's method. If our linkage is mobile, we expect from our experience with Möbius kaleidocycles that it should have a configuration where the first and second link midlines t_i form an angle of $\theta_1 = 0$. So let $f(\alpha')$ be the smallest twist angle for the other links where it is possible to build the linkage such that $\theta_1 = 0$. And let $g(\alpha')$ be the smallest twist angle without imposing that constraint. Then if we define $s(\alpha') = g(\alpha') - f(\alpha')$, we will have $s(\alpha'_c) = 0$, as we wanted. This, however, is not guaranteed as it is not necessarily the case that a mobile mechanism should go through a configuration where $\theta_1 = 0$. We may also encounter situations where the configuration with the smallest twist angle we find just happens to satisfy the constraint $\theta_1 = 0$. In short, the proposed method is fallible. However, the zeros of s are reasonable guesses to check for mobility.

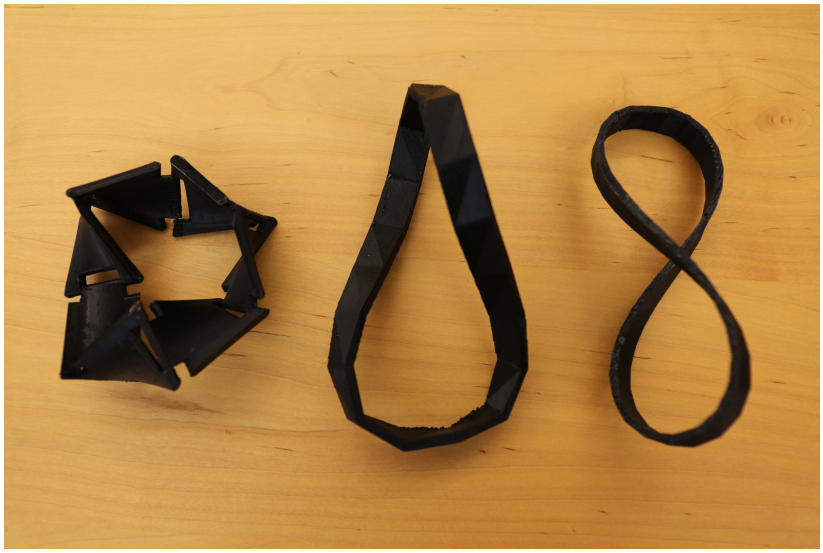

Figure 5: 3D-printed Bernoulli kaleidocycles with 7, 17 and 31 links. The 7-link one has actual hinges and can be everted, but the other ones have been 3D-printed into a particular configuration and do not have hinges because of technical limitations. As N grows, the linkages tend towards a planar lemniscate. The shown objects were designed and printed by Michael Grunwald.

Using s we find that there seem to be two solutions for α_c' of opposite sign for any $l' < l$, and with more numerical analysis we see that they actually feature a single degree of freedom. For now we only look at the positive value. Surprisingly it appears to satisfy the equation $\sin \alpha_c' = \frac{l'}{l} \sin \alpha_c$, which we write more suggestively as

$$\frac{\sin \alpha_c'}{\sin \alpha_c} = \frac{l'}{l} \tag{2}$$

to remind us of Snell's law of refraction. It predicts that there are solutions for α_c' up to a certain l'_{max} for which $\alpha_c' = \pi/2$. It is not easy to compute l'_{max} because α_c depends on l'.

We now reconsider our original system of equations (1). Changing the length of a link affects (1.3), while changing its twist angle affects (1.2) and (1.3). It turns out that if we change the length and twist angle of a link according to (2), (1.3) remains intact, so that when altering (1) we only need to change the first ($i = 1$) equation of (1.2) to:

$$h_1 \cdot h_2 = a'.$$

3.2 Bernoulli kaleidocycles

The choice $\alpha_c' < 0$ means that the disparate link will have the opposite chirality. If we take this link to have the same length but the opposite chirality, there is now a critical twist below which the chain cannot be closed *orientably* (orientability demands that the minus sign in equation (1.4) is removed), which gives another family of kaleidocycles with one degree of freedom. Here are some of their properties:

- In the limit $N \to \infty$ the midpoint curve appears to approach a lemniscate.
- If we require that the linkage evolve at a constant configuration space speed, we can graph the angles θ_i along the motion of the linkage. We find that the hinge angles θ_i for hinges connecting two equal links all follow the same evolution except for a change of phase. If the motion has period T, then the phase difference is $T/(N-2)$.

- The hinge angles of the hinges connecting the disparate link to its neighboring links have the same phase difference of $T/(N-2)$ between them, but their evolution is different from the other hinge angles.
- The system has two symmetric configurations.

It is also permissible to change the length and critical twist angle of the disparate link according to (2). The limit $\alpha_c' = \pi/2$ is a case that we can also get to from an irregular kaleidocycle without links of opposite chirality. For this choice the discrete curve does not have a defined 2π-twist topology, as a link with twist angle $\alpha = \pi/2$ does not have a defined chirality.

If $\alpha_c' = 0$, the resulting linkage is planar. In the limit $\alpha_c' \to 0$, the linkage goes towards a planar discrete linkage in the shape of a discrete lemniscate while preserving its one-dimensional motion. It is possible to study this linkage's motion in this limit, as opposed to the $(N-3)$-dimensional motion it would have in the non-limit case $\alpha_c' = 0$. This planar curve can be thought of as a discrete elastic curve, as we discuss in Section 5.3.

3.3 Irregular kaleidocycles

It is natural to ask whether it is possible to use (2) to look for kaleidocycles made from chains consisting of more than one disparate link. This leads to 3π-twisted mechanisms that evert in a similar way to a Möbius kaleidocycle, but in an irregular fashion. These kaleidocycles are fully determined by the maximal ordered sequence $(a_i) = (\cos\alpha_i)$ and they follow the system of equations

$$\begin{cases} h_i \cdot h_i &= 1, & (1.1) \\ h_i \cdot h_{i+1} &= a_i, & (1.2') \\ \sum_{i=1}^{N} h_i \times h_{i+1} &= 0, & (1.3) \\ h_{N+1} &= -h_1. & (1.4) \end{cases} \tag{1'}$$

Here (1.1) holds for $i = 1, \cdots, N+1$ and (1.2) holds for $i = 1, \cdots, N$. By maximal we mean that there is no linkage satisfying the modified system (1′) if we increase any a_i. We find numerically that such linkages have the following two nontrivial properties.

- For any irregular kaleidocycle, there exists an irregular kaleidocycle for any permutation of the same links.
- Upon a reordering that leaves a_{i-1} and a_i as before, the maximum hinge angle θ_i does not change.

We will use the following theorem to establish these properties.

3.4 The transposition theorem

Theorem: Given two consecutive links following (2) the terminal hinges of which are connected to a chain, there exists a configuration where the two links have been swapped but all remaining links remain as before. The hinge angle between the two swapped links is kept constant.

Proof: In the initial configuration we have two links with terminal hinges h_1, h_3, a connecting hinge h_2 and a midline path of $v = h_1 \times h_2 + h_2 \times h_3$ according to (2). We show that there is a rotation that takes $h_1 \mapsto -h_3, h_3 \mapsto -h_1$, and $v \mapsto -v$.

The function we are looking for is the π-rotation R_m about the axis $m = h_3 - h_1$. When acting on some vector with parallel and perpendicular components $v = v_{||} + v_{\perp}$ with respect to axis l, π-rotations act like $R_m(v) = v_{||} - v_{\perp}$. If we decompose our terminal hinge vectors in this manner we find that

$$h_1 = -\frac{1}{2}(h_3 - h_1) + \frac{1}{2}(h_3 + h_1),$$

$$h_3 = +\frac{1}{2}(h_3 - h_1) + \frac{1}{2}(h_3 + h_1),$$

from which it is clear that $R_m(h_1) = -h_3$ and $R_m(h_3) = -h_1$. Finally, notice that $v = h_2 \times (h_3 - h_1)$, which means v is perpendicular to l, and so $R_m(v) = -v$, thereby concluding the proof.

Remark: Because we have our system (1) in configuration space, we have only concerned ourselves with how the hinge vectors change. However, it is worth mentioning that the midpoint p_2 of hinge h_2 is transformed by a π-rotation around the axis in the direction $h_3 - h_1$ that goes through the point $(p_1 + p_3)/2$.

Corollary: For any irregular kaleidocycle, there exists an irregular kaleidocycle for any permutation of the same links.

Proof: Let $(a_i) = (\cos \alpha_i)$ be a maximal ordered sequence. Given any configuration of the a linkage with twist angles (α_i), any two adjacent links can be exchanged in accord with the theorem. This amounts to exchanging a_i with a_{i+1}, yielding another ordered sequence (a'_i). Granted that we can repeat this procedure any number of times, and that the set of adjacent transpositions generates the set of permutations, it follows by induction that any permutation (a^*_i) is reachable through this procedure.

To constitute an irregular kaleidocycle, a linkage must also be critically twisted. Suppose after reordering we get a non-critically twisted linkage, such that we may increase some of its twist angle cosines a'_i and still find configurations. Suppose that is done and then the transposition theorem is used to return to the original ordering. This would, however, diminish the total twist of the original irregular kaleidocycle, which is a contradiction.

Corollary: Upon a reordering that leaves a_{i-1} and a_i as before, the maximum hinge angle θ_i does not change.

Proof: Suppose $\theta_{i,\max}$ depends on the order of the other links, so that, without loss of generality, there are two sequences (a_i) and (a'_i) that are permutations of each other and for which $\theta_{1,\max} > \theta'_{1,\max}$. Take a configuration of hinges that satisfies the kaleidocycle equations for (a_i) such that $\theta_1 > \theta'_{1,\max}$, $a_1 = a'_1$ and $a_2 = a'_2$. Leave the first and second link untouched while reordering the rest according to our theorem, and get to the permutated sequence (a'_i). Now, $\theta'_1 = \theta_1 > \theta'_{1,\max}$, which is a contradiction.

Remark: We now go back to our proof of the theorem and notice that the mapping that takes (h_1, h_3) to f_{h_1,h_3} is in $SO(3)$ so it is continuous, as it is simply the rotation defined such that $f_{h_1,h_3}(h_1) = -h_3$ and $f_{h_1,h_3}(h_3) = -h_1$. Since f_{h_1,h_3} is continuous, then the function $f : (h_1, h_2, h_3) \mapsto (h''_1, h''_2, h''_3)$ must also continuous. Moreover, since f is its own inverse, it is a homeomorphic function. This has the consequence that that the solution sets in configuration space have the same topological structure for any permutation of links.

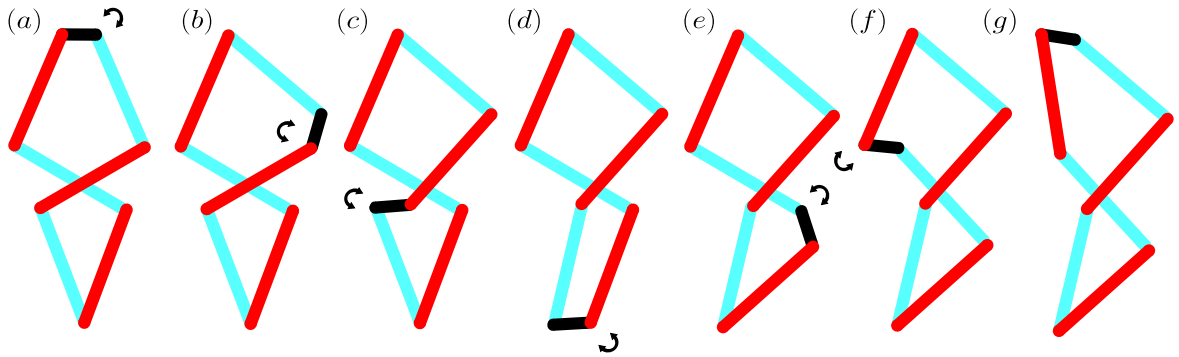

Figure 6: An illustration of a transposition cycle in 2D. In a linkage where the black link has a different length, we swap it iteratively with all other links so that in (g) we have the same link ordering as in (a), but the configuration is different. A transposition cycle is only possible in 3D when all adjacent transpositions are possible, which happens when equation (2) is satisfied for all links.

Remark: We are working in hinge space, which is homogeneous, meaning that we don't need to consider the axes of rotation in the actual mechanism. However, those axes might be useful to know. Let the midpoints of the hinges be denoted p_i. Then the rigid motion we are looking for is the π-rotation that goes through $(p_1 + p_3)/2$ with direction $m = h_3 - h_1$. We can use this to find the position of p_2 after the transposition.

3.5 An unlikely coincidence

We now take a moment to ponder the following fact: We have discovered (2) numerically by attempting to find mobile underconstrained mechanisms. This condition turned out to be the exact condition we needed for our transposition theorem. It is therefore natural to seek a relationship between mobility and the operation of transposing consecutive links. What follows is a plausibility argument for the mobility of irregular kaleidocycles, including Möbius kaleidocycles. Underlined statements would need to be made rigorous and proved to make the following argument rigorous.

In any irregular kaleidocycle, we can transpose the first link with the second, then the second with the third, and so on, until we arrive at the same ordering of the links as in the beginning. We call this a *transposition cycle*. This cycle produces a new configuration for this ordering.

Given an irregular kaleidocycle, we can add a link of length $l' \ll l_i$, $i = 1, \cdots N+1$ and readjust the twist angle very slightly to make it critical. This readjustment becomes negligible as $l' \to 0$. Now, a transposition cycle of the small link through the ring will yield a configuration that is very close to the original one. By performing this cycle again and again we will keep visiting new configurations. As $l' \to 0$, this discrete collection of new configurations will translate into a continuous, finite degree of freedom.

If this transposition cycle is performed numerically with a small link, we can observe the motion of the linkage. While there is no proof that Möbius kaleidocycles are mobile, this plausibility argument is the best explanation we have for this numerically observed phenomenon at this time. Transposition cycles are also interesting on their own as they give rise to discrete surfaces with special properties, as we discuss in Section 5.

4 Open chains

Now we return to equal twisted links, as we are interested in another generalization. Instead of a closed loop, we will take the first and last hinge midpoints to be separated by some fixed distance L. If we do not restrict the orientations of the first and last hinges, once we find the critical twist angle α_c, we numerically find that our mechanical chain has no degrees of freedom.

However, if we restrict the first and last hinges to be antiparallel (namely if we retain equation (1.4)), we do find interesting solutions with one degree of freedom. This condition is natural for closed chains, but it is not obvious why it is needed now. Later we give a version of transposition cycles that works for open chains using this condition. Our new system of equations is

$$\begin{cases} h_i \cdot h_i &= 1, & (1.1) \\ h_i \cdot h_{i+1} &= a, & (1.2) \\ \sum_{i=1}^{N} h_i \times h_{i+1} &= Le_1, & (1.3'') \\ h_{N+1} &= -h_1, & (1.4) \end{cases} \qquad (1'')$$

where only (1.3) has been changed and the vector connecting the terminal hinge midpoints is directed along the x-axis. A technical point arises now as to whether equation (1.4) is a kinematic pair, and by extension, whether the complete chain is a kinematic chain in the traditional sense defined, for example, by Angeles [1], when (1.4) is included. Regardless, we will for brevity continue calling these systems open chains.

According to our system $(1'')$ vectors h_1 and h_{N+1} may be in any point on the sphere $\mathbb{S}^2 \subset \mathbb{R}^3$, but that includes rigid rotations of the whole chain around the x-axis, which are of no interest. In practice, we restrict the terminal hinges to parallel planes when constructing the chain. Now we consider the situation of the terminal hinges being restricted to a common plane. This plane is assumed to include the x-axis, and we arbitrarily use the xy-plane, thus fixing an xyz-frame and a corresponding orthonormal basis (e_1, e_2, e_3). We explore what happens when we restrict the terminal hinges to different planes later.

The perpendicular configuration exhibited in Figure 7, where the terminal hinges are parallel to the y-axis, seems to be possible for any $L \in [0, N] \subset \mathbb{R}$. We take γ to be the angle that the first hinge makes with the positive y-axis. For each N and L, we typically find a limit angle $\gamma_c \in [0, \pi/2)$. It is impossible for the terminal hinges to move beyond this angle while satisfying system $(1'')$.

However, for any particular number $N \geq 5$ of links, there appears to be a finite number of chains MWN_i, $i = 1, \cdots, k$ with corresponding lengths L_{MWN_i} and twist angles $\alpha_{MWN_i}$for which γ_c does not exist and the chain can rotate indefinitely. For instance, for $N = 5$, we have found two lengths L that permit this indefinite rotation of the terminal hinges. We are interested especially in the mechanisms that correspond to these critical lengths. Our first reason for this is that a mechanism that can fully rotate might be valuable for applications. A second reason is that the finiteness of solutions is interesting in itself.

We can rotate the terminal hinges in an N-link open chain MWN_i, $N \geq 5$, at constant angular speed, giving a natural description of the movement of the chain, which we can parametrize simply by the rotation angle γ with respect to the y-axis.

4.1 Transpositions and mobility

Removing the first link and placing it after the last link by connecting it to the last hinge without altering its orientation, we still obtain a solution to $(1'')$ with the same links and length L. We call

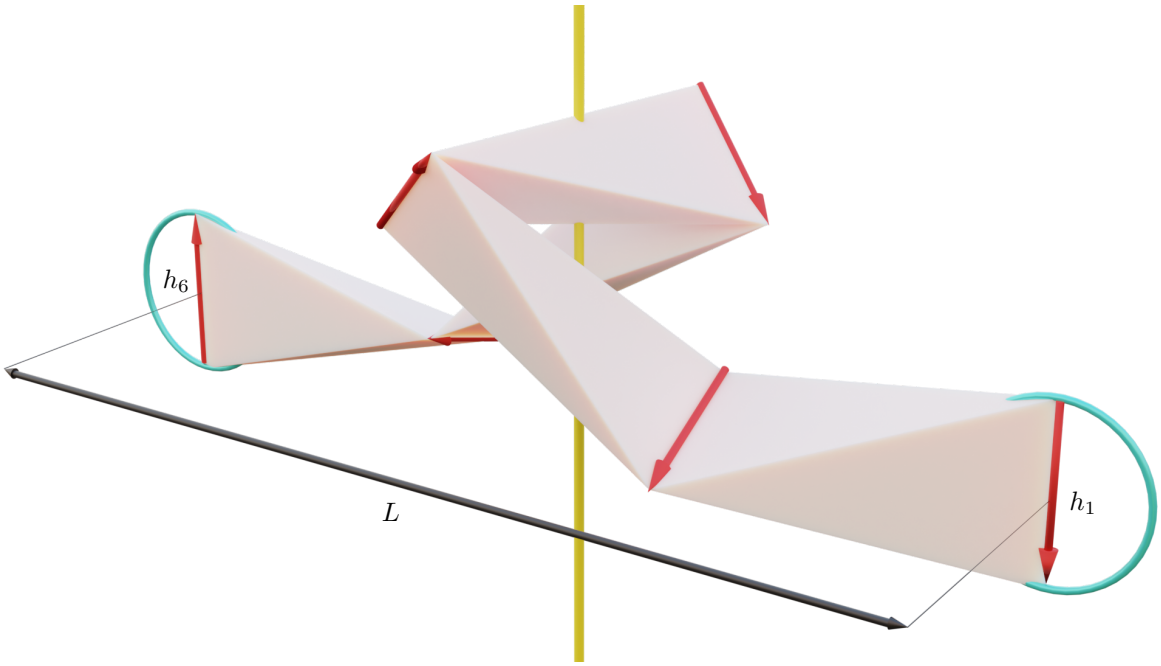

Figure 7: A 5-link open chain with $L = L_{MW5_1} = 2.89793$ and critical twist angle $\alpha_c = 0.4008\pi$. In this setup, the terminal hinges h_1, h_6 are restricted to the blue circles. This chain is shown in a perpendicular configuration, where it is symmetric under a π-rotation around the y-axis shown in yellow.

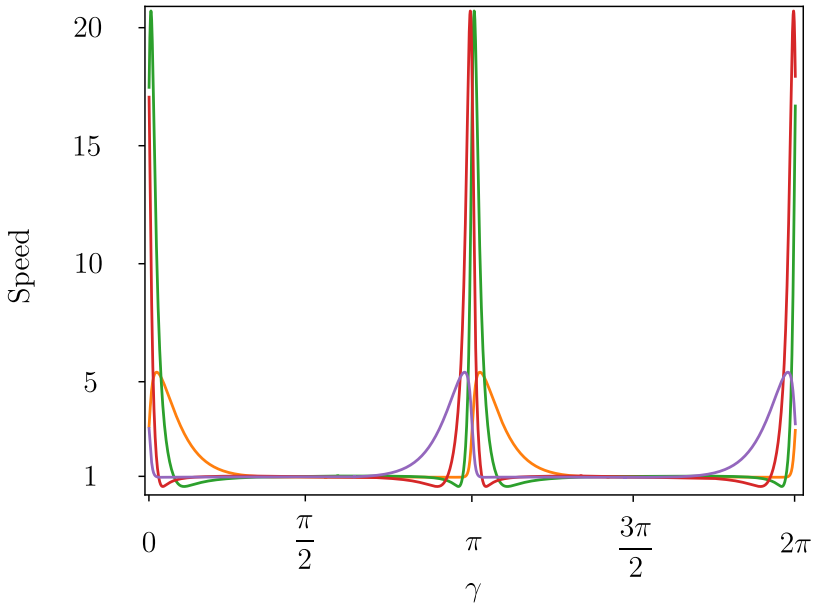

Figure 8: The speed of the hinge midpoints p_i, $i = 2, \cdots, 5$ in a 5-link open chain $MW5_1$ as we move γ with a constant angular speed of $\dot{\gamma} = 1$, excluding the terminal hinge midpoints which are held fixed. The speeds of p_2 and p_5 are in orange and purple, while those of p_3 and p_4 are in green and red. When $\gamma = 0$, we are in the perpendicular configuration. As we can see, the midpoints p_i typically travel at a common natural speed of $v = \dot{\gamma} l_i = 1$ as we vary γ, but the speed of each p_i increases significantly near the perpendicular configuration. The midpoints p_3 and p_4 can go more than 20 times faster than the standard speed.

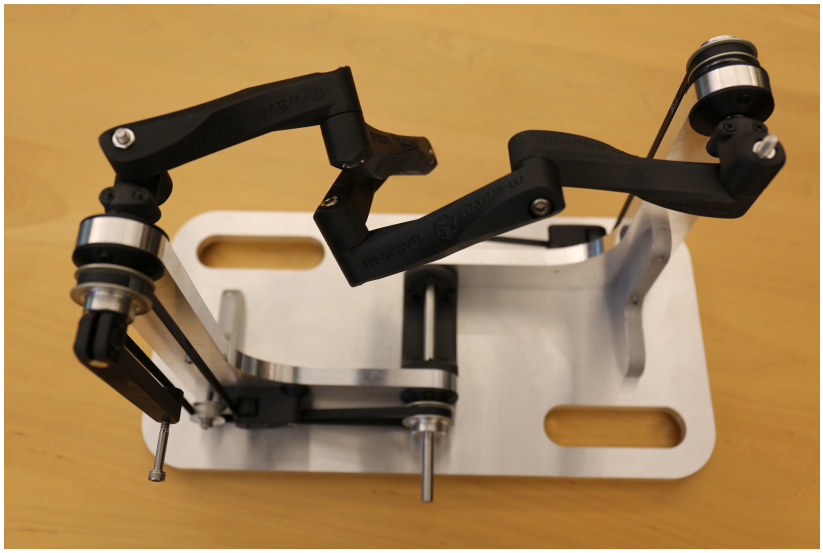

Figure 9: A physical realization of a 5-link fully rotating open chain. This device was designed and built by Michael Grunwald. The support structure holds the terminal hinges parallel throughout the motion, which can be controlled with a handle.

this operation a *link jump*. With this in mind, it is expected that, despite the asymmetry of the system, all the maximum hinge angles $\theta_{i,max}$ are all the same, as we can reorder them using link jumps. This is consistent with our numerical results. Notice that we can only do this because the first and last hinges are (anti-)parallel. This operation is what motivates us to enforce equation (1.4) even though the chain is not closed.

Nothing keeps us from making irregular open chains from disparate links, as long as we follow (2) when choosing lengths and twist angles. We can make the same argument applied to determine the mobility of an open chain that was given in Section 3.5 for kaleidocycles. The underlying transposition cycle is now a bit different, however. Starting with the small link, we transpose it with all the links in one direction until we reach a terminal hinge. We now take a link jump. Finally we transpose it again with the other links until we reach the original ordering. Since the condition (1.4) is needed for the link jump, it should not be surprising that minimizing the twist angle α without including this equation yields immobile chains. As in Section 3.5, this is merely a plausibility argument, not a rigorous proof, for mobility.

4.2 Symmetric configurations

Open chains which can fully rotate exhibit symmetry in two different configurations: The coaxial configuration, where the terminal hinges are aligned with the x-axis, and the perpendicular configuration, in which the hinge vectors are perpendicular to that axis. We have empirically found the following two symmetries.

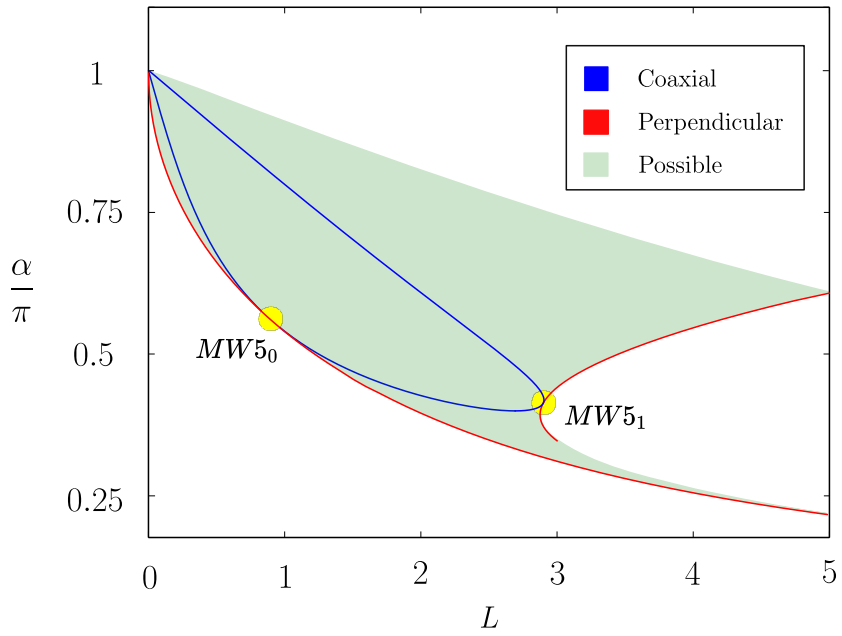

Figure 10: Symmetry α vs. L graph for a 5-link open chain. In green are all possible solutions. Perpendicular solutions appear to all lie on the boundary of all possible configurations. The two tangential intersection points of the coaxial solutions with the boundary represent a fully rotating open chain. We find $MW5_0$ at $(\alpha, L) = (0.5501\pi, 0.903)$ and $MW5_1$ at $(\alpha, L) = (0.4008\pi, 2.8979)$. Only $MW5_1$ generalizes to $N > 5$. There is another solution at $(\alpha, L) = (\pi, 0)$, but it is planar.

- **Coaxial configuration symmetry:** For a system with $N+1$ hinges, if $h_i = (a_i, b_i, c_i)^T$, then $h_{N+2-i} = (-a_i, -b_i, c_i)^T$.
- **Perpendicular configuration symmetry:** For a system with $N+1$ hinges, if $h_i = (a_i, b_i, c_i)^T$, then $h_{N+2-i} = (a_i, -b_i, c_i)^T$. For even N, we also require $h_{\frac{N+2}{2}} = (\pm 1, 0, 0)$.

Remember that we are using an orthonormal frame where the x-axis is in the direction of $p_{N+1} - p_1$ and the terminal hinges are restricted to the xy-plane. From now on when we speak of a coaxial or a perpendicular configuration, we mean one possessing one of the symmetries listed above. Numerical methods can be used to find symmetric solutions to system $(1'')$ and look for points of critical torsion where there is a coaxial and a perpendicular configuration. We draw α vs. L graphs by highlighting the regions where the open chain can reach the required symmetric configurations. We then look for points where the boundary of the symmetry configurations intersects the boundary of all possible points. To illustrate this approach, it is instructive to consider the simplest cases. In particular, $N = 5$ and $N = 6$ are a nice starting point since the solution sets for the coaxial and perpendicular configurations form one-dimensional α vs. L plots.

The coaxial-perpendicular equivalence for even N: For N even, we numerically find that the coaxial and perpendicular configurations fill exactly the same points in α vs. L space, which means an open chain has a coaxial configuration if and only if it has a perpendicular configuration. We next give an explanation of this phenomenon.

Consider an open chain with even N in a coaxial configuration. Then, $h_{\frac{N+2}{2}} = (\pm 0, 0, \pm 1)$. Now, we perform a link jump for every link in the first half of the chain, so that $h_{\frac{N+2}{2}}$ becomes h_1', which is perpendicular to $(1, 0, 0)$, so we get a perpendicular configuration for the same chain. Starting with a perpendicular configuration, a coaxial configuration can be achieved by an analogous procedure.

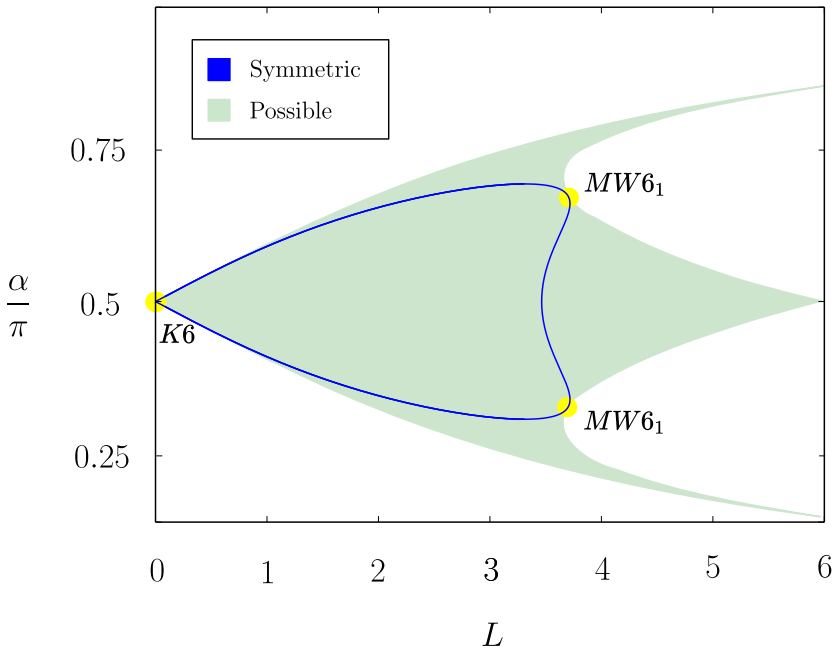

Figure 11: Symmetry α vs. L graph for a 6-link open chain. Coaxial and perpendicular configurations are equivalent for even N so we have grouped them under the term *symmetric*. The symmetry of the graph with respect to the line $\alpha = \pi/2$ is apparent. The points of interest are $K6$, which refers to the classical kaleidocycle, at $(\alpha, L) = (\pi/2, 0)$, and $MW6_1$ at $(\alpha, L) = (0.3349\pi, 3.694)$, an open chain with 6 links.

The symmetry between $\alpha = \pi/2 - x$ and $\alpha = \pi/2 + x$: For N even, the transformation $\alpha = \pi/2 - x \mapsto \pi/2 + x$ amounts to a change of chirality, so the α vs. L graphs are symmetric with respect to the line $\alpha = \pi/2$. For odd N, the transformation $\alpha = \pi/2 - x \mapsto \pi/2 + x$ changes the sign of the last hinge, so the symmetry is destroyed. Because of this, for odd N the upper half of the α vs. L graph is symmetric to the lower half of an analogous graph where the terminal hinges are parallel instead of antiparallel. For even N, because of the symmetry, configurations with parallel terminal hinges do not appear in the usual α vs. L graph, so that if we want to find all fully rotating open chains, we need to also examine the analogous graph with parallel terminal hinges.

Solutions with $L = N$: A fully stretched out chain (all $\theta_i = 0$) has length $L = Nl = N$. For it to satisfy (1.4), we need $N\alpha_s^* = (2k+1)\pi$ for some $k \in \mathbb{Z}$. The number of $\alpha_i^* \in [0, \pi]$ satisfying this equation is $\lfloor N/2 \rfloor$. This accounts for the "teeth" observed in the right side of the possible α vs. L graphs. They go from some α_i^* to α_{i+1}^*. We conjecture that the only proper ($L > 0$) fully rotating open chain that doesn't lie on a tooth is $MW5_0$ and that there is exactly one fully rotating open chain for every tooth. These appear to all display a similar movement and properties, but vary in speed and size of the wave. From this we would expect that for smooth curves ($N \to \infty$) there will be a countable infinity of fully rotating open chains at quantized lengths. Indeed, this has been described by Ivey [6].

An open chain that can rotate by half a revolution: There is a chain for $N = 5$ at $(\alpha, L) = (0.6445\pi, 1.766)$. While the other open chains we have found can either do a full revolution or rotate up to $\gamma_c < \pi/2$, this open chain can undergo a rotation up to $\gamma_c = \pi$, and cannot move towards negative γ. The chain features a movement that appears to be qualitatively different from that of the other studied chains and instead of lying on a tooth, it lies on the top edge of all possible configurations.

4.3 Tilted open chains

When we construct an open chain we restrict h_1 and h_{N+1} to each lie in a plane throughout the motion. These two planes must be parallel, but may differ otherwise. If the planes are not the same, or equivalently, if they do not include the x-axis, we say we have tilted planes, or a tilted open chain. The tilt angle $\beta \in [0, \pi/2]$ is the angle the plane makes with the x-axis. The lower limit $\beta = 0$ corresponds to a non-tilted cutting plane. The upper limit $\beta = \pi/2$ corresponds to a perpendicular cutting plane. The latter is the least interesting of all admissible choices for β, as the motions it admits are rigid rotations.

There are many practical reasons why it might be preferable to build a tilted open chain. First, tilted chains don't go through a coaxial configuration. In the coaxial configuration, a chain can undergo rigid rotations around the x-axis, which is likely undesired behavior when the terminal hinges are fixed on a plane. Furthermore, as we have seen, the number of fully rotating open chains MWN_i seems to be finite for any $N \geq 5$. Chains where terminal hinges can undergo a full revolution might be useful as one can drive them easily with a handle or a motor. But the small number of fully rotating open chains limits design freedom, where it is desirable to have as many free parameters as possible.

For a not fully rotating open chain with some γ_c, a tilt angle that allows the terminal hinges can fully rotate must satisfy $\beta \in [\gamma_c, \pi/2]$. For $\beta = \gamma_c$, we find empirically that the system can move in two different ways (there is a crossover at the perpendicular configuration). One of which undergoes an extra rotation around the x-axis. Choosing $\beta = \gamma_c$ and the movement that doesn't have this extra rotation appears to give solutions where $h_1 \times h_2$ and $h_N \times h_{N+1}$ each lie within a hemisphere, which makes it possible to construct a support structure for the chain.

4.4 Axis of symmetry

The symmetry axis of a Möbius kaleidocycle is very easy to find when N is a multiple of 3. In these cases the linkages are threefold symmetric around an axis, which we may identify as the symmetry axis. When N is not a multiple of 3 the problem of identifying a symmetry axis is harder. Schönke and Fried [4] prescribe the axis from the start and require that the hinges and midpoints all follow the same movement, apart from a rotation about the symmetry axis and a change of phase. Fourier analysis can then be used to find these paths from a starting position.

For irregular kaleidocycles and open chains, none of the above methods can be used to find the symmetry axis, so we need to find other properties of this axis in order to find it.

The axis of an open chain: An open chain with a very small L can be arbitrarily close enough to a kaleidocycle. In the limit $L \to 0$, numerics suggest that $Le_1 = p_{N+1} - p_1 = \sum h_i \times h_{i+1}$ is parallel (but not equal) to the axis. So the direction of the axis of symmetry may be well-defined for irregular kaleidocycles, and can be found with an infinitesimal transformation. Moreover, it is sensible to say that the symmetry axis of an open chain, if it exists in some sense, is parallel to the vector connecting the terminal hinges. We discuss this further in the next section.

5 Discrete differential geometry

This section provides a window to the relationship between the research discussed in this thesis and the field of discrete differential geometry. It is more of an avenue for further research than a description of results.

5.1 Introduction

Discrete differential geometry is not a standard topic in undergraduate or graduate mathematics, so here we give some definitions and statements without proof, adapted from the book of Bobenko and Suris [7]. For functions on $\mathbb{Z}^m$, we use the notation $\tau_i f(u) = f(u+e_i)$, where e_i is the i-th coordinate vector of $\mathbb{Z}^m$.

Definition 1: A map $f : \mathbb{Z}^m \to \mathbb{R}^N$ is called an m-dimensional *Q-net* (discrete conjugate net) in $\mathbb{R}^N$ if all its elementary quadrilaterals are planar, namely, if at every $u \in \mathbb{Z}^m$ and for every pair $1 \le i \ne j \le m$ the four points $f, \tau_i f, \tau_j f$ and $\tau_{ij} f$ are coplanar.

We are particularly interested in one type of Q-nets.

Definition 2: A map $y : \mathbb{Z}^3 \to \mathbb{R}^N$ is called an m-dimensional *T-net* if for every $u \in \mathbb{Z}^m$ and for every pair of indices $i \ne j$, the discrete Moutard equation with minus signs,

$$\tau_i \tau_j y - y = a_{ij}(\tau_j y - \tau_i y), \tag{3}$$

holds with some $a_{ij} : \mathbb{Z}^m \to \mathbb{R}$. In other words, if all elementary quadrilaterals $(y, \tau_i y, \tau_j y, \tau_{ij} y)$ are planar and have parallel diagonals.

Now we look at a class of discrete surfaces defined in a different way.

Definition 3: A map $f : \mathbb{Z}^m \to \mathbb{R}^3$ is called an m-dimensional discrete *A-net* (discrete asymptotic net) in $\mathbb{R}^3$ if for every $u \in \mathbb{Z}^m$ all the points $f(u \pm e_i)$ lie in some plane $\mathcal{P}(u)$ through $f(u)$.

Discrete A-surfaces serve as discrete counterparts of surfaces parametrized along their asymptotic lines. The tangent plane $\mathcal{P}(u)$ also defines a normal direction.

Theorem 1: For a nondegenerate discrete A-net $f : \mathbb{Z}^m \to \mathbb{R}^3$, there exists a normal field, called a *Lelieuvre field*, $n : \mathbb{Z}^m \to \mathbb{R}^3$ such that

$$\tau_i f - f = \tau_i n \times n. \tag{4}$$

This field is uniquely defined by a value at one point $u_0 \in \mathbb{Z}^m$. All other Lelieuvre normal fields are obtained by a transformation of the form $n(u) \mapsto \alpha n(u)$ for $|u| = u_1 + \cdots + u_m$ even, and $n(u) \mapsto \alpha^{-1} n(u)$ for $|u| = u_1 + \cdots + u_m$ odd, with some $\alpha \in \mathbb{R}$. A transformation of this form is called a *black-white rescaling*.

Theorem 2: Discrete A-nets in $\mathbb{R}^3$ (modulo parallel translations) are in one correspondence, via the discrete Lelieuvre representation, with T-nets in $\mathbb{R}^3$ (modulo black-white rescalings).

We are especially interested in the following A-nets, which are discrete counterparts of surfaces with constant negative Gaussian curvature.

Definition 4: A discrete A-net $f : \mathbb{Z}^m \to \mathbb{R}^3$ is called an m-dimensional discrete *K-net* if for any elementary quadrilateral $(f, \tau_i f, \tau_j f, \tau_{ij} f)$,

$$|\tau_i \tau_j f - \tau_j f| = |\tau_i f - f| \text{ and } |\tau_i \tau_j f - \tau_i f| = |\tau_j f - f|. \tag{5}$$

Theorem 3: The Lelieuvre normal field $n : \mathbb{Z}^m \to \mathbb{R}^3$ of a discrete K-net $f : \mathbb{Z}^m \to \mathbb{R}^3$ takes values, possibly upon black-white rescaling, in some sphere $S^2 \subset \mathbb{R}^3$, thus being proportional to the Gauss map.

5.2 K-nets in critically twisted mechanisms

In the continuous limit, K-nets become K-surfaces, which have constant negative Gaussian curvature. The asymptotic lines of a K-surface have constant torsion. So asymptotic lines of discrete surfaces can be viewed as a discrete counterpart to curves of constant torsion. Our irregular chains can be seen as discrete curves, and equation (2) says they agree with Theorem 3 above, making them asymptotic lines of some K-surface. In this way, our chains are discrete curves of constant torsion. We now describe a particularly interesting way to construct a K-net from an irregular chain.

Let us start with an irregular kaleidocycle or an irregular critically twisted open chain. We do a transposition cycle of the first link. Each time we swap the links i and $i+1$ connecting hinges h_i, h_{i+1}, and h_{i+2} we move $h_{i+1} \mapsto h'_i$, and $p_{i+1} \mapsto p'_i$ according to the last remark in Section 3.4 and $h_1 \mapsto h'_N$. We have relabeled the hinges so after the full cycle the i-th link still connects hinges h'_i and h'_{i+1}.

Now, note $h'_2 \cdot h_2 = h_1 \cdot h_2 = a_1$ and also that $p_2 - p'_2 = p_2 - p_1 = h_1 \times h_2 = h'_2 \times h_2$. Moreover, we can perform the first transposition in the cycle and continue from there, inferring that $h_3 \times h'_3 = a_1$, that $p_3 - p'_3 = h'_3 \times h_3$, and by an inductive argument, the same follows for any hinge. Therefore, in the discrete motion given by transposition cycles, each hinge midpoint is moved along a discrete curve of constant twist. Combining these observations, we arrive at the following

Proposition: Let f_{ij} denote the midpoint p_i of hinge i after j transposition cycles. Then f is a discrete K-surface, and the Gauss map of f represents the hinges h_{ij}.

K-nets and the axis of symmetry: The K-nets of Möbius kaleidocycles with a very small link added appear to go in the direction of the axis of symmetry on passing to the limit $M \to \infty$ of an infinite number of transposition cycles. Moreover, when the kaleidocycle has undergone a full eversion, it has also rotated a certain amount around that axis. This rotation demands an axis and not only a direction, which means we can determine the position of the axis. This is so far the only way we have found of computing the symmetry axis for irregular kaleidocycles and open chains, as it is the only concrete meaning we have been able to assign to the symmetry axis in these cases.

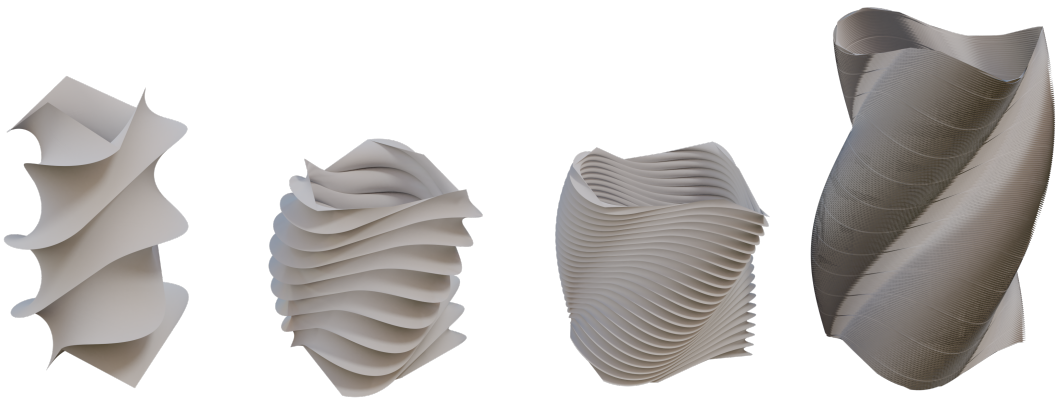

K6 MK9 MK12 MK30

Figure 12: Semidiscrete K-surfaces for Möbius kaleidocycles. These surfaces have been constructed by adding a very small link to the linkage with a twist angle according to (2) and performing successive transposition cycles. The limit as $N \to \infty$ is a smooth K-surface with periodicity in the vertical direction and the topology of a cilinder.

5.3 Discrete elastic curves

An elastic curve is $\gamma : \mathbb{R} \to \mathbb{R}^3$ minimizing the bending energy functional $\int_0^L \kappa^2 dl$, where κ is the usual curvature and L is the length of the curve. Two-dimensional elastic curves were studied by Jacob Bernoulli and they were later classified by Euler. [8]

Curves that minimize the functional $\int \kappa^2 + c\tau^2$ for some $c > 0$ are of some further interest to us. These curves are typically referred to as elastic rods in the literature, but we will abstain from using this term, as the curves don't describe the mechanics of physical elastic rods. As $N \to \infty$ with each $l_i \to 0$, critically twisted chains following (2) become curves of constant, critical torsion. Ivey [6] presents the following

Theorem: Any smooth curve which is critical for arclength, with respect to variations among curves of a fixed nonzero constant torsion, fixing the Frenet frame at the endpoints, must be either a minimizer of the aforementioned functional.

This applies to our chains when $N \to \infty$. So for instance, if we assume that Bernoulli kaleidocycles become planar as $N \to \infty$, they tend towards a closed planar elastic curve. There are only two of these (modulo uniform dilations), and in this case the limiting curve appears to be the lemniscate, the other class of two-dimensional elastic curves being composed of circles.

Now we look at the discrete case. It was already noted by Schönke and Fried [4] that $\sum_{i=1}^N \theta_i^2$ is very close to being constant along the motion of Möbius kaleidocycles. In fact, if we use the definition of bending energy given in [9] for arclength-parametrized discrete curves, namely

$$E = \sum_{i=1}^{N} \log(1 + \tan^2 \theta_i/2), \tag{6}$$

we find analytically that the classical kaleidocycle has a constant elastic energy of $6 \log 2$. For Möbius kaleidocycles we can numerically confirm that they also have constant elastic energy. For open chains we need to also consider the angle θ_0 between the first and last link, but the result is identical. While the analogous results for smooth curves were derived by Euler, the classification problem for discrete planar elastic curves seems to be unsolved as of this time. This requires a satisfactory definition for the curvature and bending energy of a discrete non-arclength parametrized curve that is analogous to (6), which corresponds to a curvature and bending energy for chains composed of disparate links.

It is natural to conjecture that the previous theorem also holds for discrete curves, under the definition for a discrete functional given by Bobenko [9]. That is, curves that are local minima for the energy $E = \sum \log(1 + \tan^2 \theta_i/2) + c \log(1 + \tan^2 \alpha_i/2)$ for some $c > 0$.

The variational problem for smooth centerlines of elastic rods is related to the Lagrangian formulation of the Lagrange top, which is a classical problem studying the movement of a top that has rotational symmetry, with its center of mass lying on the symmetry line. This relationship is explored in more detail by Bobenko and Suris [9][10] for discrete curves and a time-discretized Lagrange top. From this perspective, the axis of symmetry of a chain is closely related to the axis of symmetry observed in the rotation of a top.

6 Conclusion

At the beginning of my stay at OIST, I was interested in theoretical questions regarding Möbius kaleidocycles. Why are they mobile? Why do they have a 3π-twist instead of a π-twist? These questions happen to be quite difficult. Moreover, Möbius kaleidocycles are very regular, which endows

them with many properties (like symmetry) that do not necessarily have anything to do with the question of interest, making those properties red herrings.

The reason for introducing irregular kaleidocycles is not necessarily that any particular irregular kaleidocycle is especially interesting in on its own (except for Bernoulli kaleidocycles in the uniform link length and the planar limit cases). Instead, this was done to provide an avenue to find more objects that behave like Möbius kaleidocycles, and thereby allow for the study of the whole class of such objects and for the discovery of common properties. From the point of view of irregular kaleidocycles, we were led to the discovery of equation (2), which is formally identical to Snell's law of refraction and seems to constitute a necessary condition for mobility of critically twisted chains. Moreover, we arrived at a first insight into the mobility of Möbius kaleidocycles through the transposition theorem.

Initially, the motivation for studying open chains might appear to be similar. However, the family of open chains appears to have a very rich structure, including many special cases that are worth studying. Much work remains to find and classify all fully rotating open chains, and there may be other open chains with interesting properties. I am also hopeful that some analytic results can be obtained, at least for the 5-link chains $MW5_0$ and $MW5_1$.

Because my findings in the direction of discrete differential geometry ocurred only late into this project, which happens to have a strict deadline, I was unable to develop the last section as much as I would have liked. However, I believe that discrete differential geometry will play a significant role in the theory of critically twisted kinematic chains, and that it will help to establish theoretically the results that we observe numerically. Conversely, critically twisted chains are an outstanding example of discrete differential geometry, and I hope a greater understanding of these chains will further advance the subject.

References

[1] J. Angeles, *Rational Kinematics*, Springer-Verlag New York, 1st edition, 1988.

[2] L.-W. Tsai and A.P. Morgan, *Solving the Kinematics of the Most General Six- and Five-Degree-of-Freedom Manipulators by Continuation Methods*, Journal of Mechanical Design, 107(2): 189–200, 1985

[3] C. Mavroidis and B. Roth, *Analysis of Overconstrained Mechanisms*, Journal of Mechanical Design, 117(1): 69–74, 1995

[4] J. Schönke and E. Fried, *Single degree of freedom everting ring linkages with nonorientable topology*, Proceedings of the National Academy of Sciences, 116(1): 90–95, 2019

[5] R. Bricard, *Leçons De Cinématique. Tome II, Cinématique Appliquée*, Gauthier-Villars Paris, 1927

[6] T. Ivey, *Minimal Curves of Constant Torsion*, Proceedings of the American Mathematical Society, 128: 2095–2103 2000

[7] A.I. Bobenko and Y.B. Suris, *Discrete Differential Geometry: Integrable Structure* American Mathematical Society, 2008

[8] Truesdell C., *The Influence of Elasticity on Analysis: The Classic Heritage*, Bulliten of the American Mathematical Society 9: 293–310, 1983

[9] A.I. Bobenko and Yu. I. Suris, *Discrete Time Lagrangian Mechanics on Lie Groups, with an Application to the Lagrange Top*, Communications in Mathematical Physics, 204: 147–188, 1999

[10] A.I. Bobenko *Geometry II: Discrete Differential Geometry*, Lecture Notes, 1999